


IADC/SPE 150461

Modeling for MPD Operations with Experimental Validation

Ingar Skyberg Landet, Hessam Mahdianfar, Ulf Jakob F. Aarsnes, NTNU; Alexey Pavlov, Statoil; Ole Morten Aamo, NTNU

Copyright 2012, IADC/SPE Drilling Conference and Exhibition

This paper was prepared for presentation at the 2012 IADC/SPE Drilling Conference and Exhibition held in San Diego, California, USA, 6–8 March 2012.

This paper was selected for presentation by an IADC/SPE program committee following review of information contained in an abstract submitted by the author(s). Contents of the paper have not been reviewed by the International Association of Drilling Contractors or the Society of Petroleum Engineers and are subject to correction by the author(s). The material does not necessarily reflect any position of the International Association of Drilling Contractors or the Society of Petroleum Engineers, its officers, or members. Electronic reproduction, distribution, or storage of any part of this paper without the written consent of the International Association of Drilling Contractors or the Society of Petroleum Engineers is prohibited. Permission to reproduce in print is restricted to an abstract of not more than 300 words; illustrations may not be copied. The abstract must contain conspicuous acknowledgment of IADC/SPE copyright.

Abstract

Heave motion of floating rigs complicates the control of pressure in MPD. During connections, the drill string is detached from the draw-works and moves with the heaving rig, causing downhole pressure fluctuations. As a step towards designing control schemes to actively attenuate the fluctuations, a fit-for-purpose mathematical model of well hydraulics is derived based on a finite volumes discretization. The model incorporates various MPD operations, including circulating in new mud, vertical motion and rotation of the drill string. Using field data from UllRigg - a full-scale experimental drilling facility - the model is validated with respect to the different MPD operations. Since an automatic control scheme in principle inherits the complexity of the model on which it is based, it is of great importance to develop models of minimal complexity. It is shown by simulations that significantly reduced order models obtained by applying the method of frequency-weighted balanced model reduction to large models outperform those obtained by simply reducing the number of control volumes. This result is particularly important for the dynamics involved during heave, since a significant number of control volumes are required to model this case. The contributions of this paper enable development of control systems for automated MPD operations from floaters.

1 Introduction

In drilling operations, a drilling fluid called mud is pumped down the drill string and flows through the drill bit in the bottom hole of the well (See Figure 1). Then it flows up the well annulus carrying cuttings out of the well. It is also used to keep the pressure in the annulus at a desired level. This pressure control is crucial in all drilling operations, as the pressure has to be between certain boundaries. Specifically, it has to be above the pore pressure to prevent unwanted inflow from the surrounding formations into the well, and below the fracture pressure of the surrounding formations to prevent the well from fracturing.

Managed pressure drilling (MPD) is an adaptive drilling process used to precisely control the annular pressure in the wellbore. The objectives are to ascertain the down-hole pressure environment limits and to manage the annular hydraulic pressure profile accordingly [1]. Controlling the annulus pressure in an oil well during drilling can be a challenging task due to the very complex dynamics of the multiphase flow potentially consisting of drilling mud, oil, gas and cuttings. By allowing manipulation of the topside choke and pumps, MPD provides a means of quickly affecting pressure to counteract disturbances. A description of the standard setup of an automated MPD system can be found for instance in [2]. The schematic of an MPD system is shown in Figure 1.

Since down-hole pressure measurements are unreliable due to slow sampling, transmission delays, and loss of communication for low or no-flow conditions, the core component in the control schemes is an estimator for the down-hole pressure. In [3], an unscented Kalman filter exploiting down-hole measurements is used to tune the predicted pressure loss due to friction in both the drill string and the annulus. In [4–6], nonlinear adaptive observers are developed based on a simple dynamic model, consisting of only three ordinary differential equations. In [7], nonlinear model predictive control in combination with an unscented Kalman filter is used to control the bottom-hole pressure based on a two-phase flow model from [8] and [9]. In [10], a switched control scheme for regulation of the annular pressure in a well during drilling is presented, that also detects and handles kicks. There is still a significant potential to improve existing control and estimation schemes [11]. To accurately estimate and control mud pressure in a given position inside the well, one needs to have an accurate model of pressure distribution along the well in various operational procedures. Hydraulic models capturing different aspects of the drilling hydraulics have been developed by

several researchers [12–26]. For MPD operations using advanced hydraulics models, see for example [27–29]. The objective of this paper is to tailor a model for the purpose of designing automatic control systems. Since an automatic control scheme in principle inherits the complexity of the model on which it is based, it is of great importance to develop models of minimal complexity. In this paper, we develop a model based on finite volumes discretization, thereby providing a means of varying complexity by selecting the number of control volumes. We analyze how the number of control volumes affects the performance of the model with respect to various operational scenarios, including

1. Circulation of different muds (changes in viscosity, density and bulk modulus).

2. Vertical motion of the drill string.

3. Rotational motion of the drill string.

4. Mud gelling (viscous friction with stiction).

Finally, we apply the method of frequency-weighted balanced model reduction and show in simulations that the resulting models of low complexity outperform those obtained by simply reducing the number of control volumes.

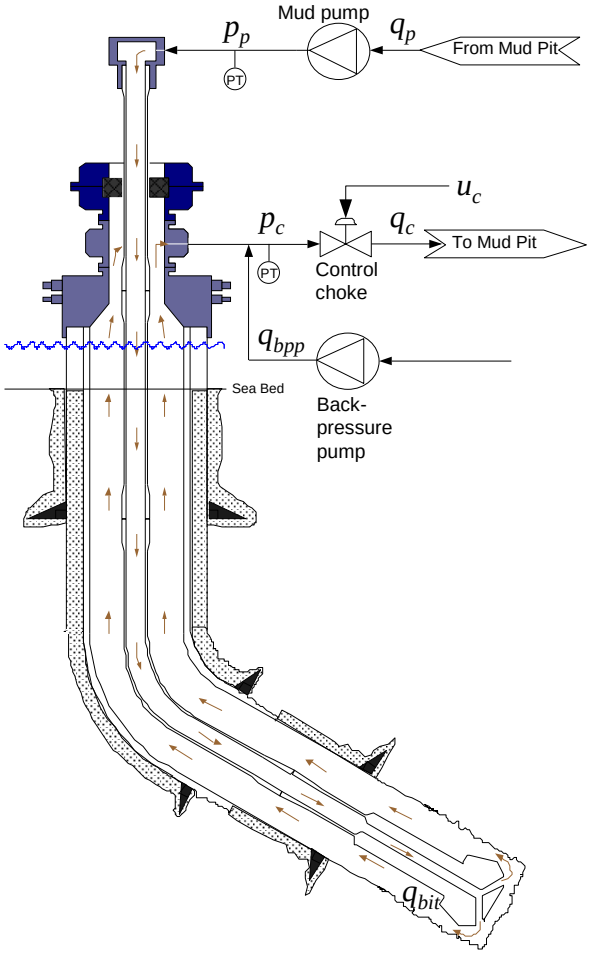

Figure 1: Schematic of an MPD system

The paper is organized as follows: In Section 2, we present mathematical modeling for MPD including the operational scenarios mentioned above. Simulation results and verification of the model using experimental data from full-scale Ullrigg rig at IRIS are given in Section 3. Section 4 provides comparison of model order reduction using frequency-weighted balanced

model reduction and reducing the number of control volumes, and finally conclusions are offered in Section 5.

2 Mathematical Modeling

2.1 Hydraulic Transmission Line

We are considering single-phase flow in both the drill string and the annulus, so the system is adequately modelled by considering it a hydraulic transmission line and follow the standard derivations in [30], pages 429-430. The hydraulic transmission line model is derived from the mass and momentum balances for a differential control volume Adx, where $A[m^2]$ is the cross section area and $x[m]$ is the spatial coordinate along the volume. The volume contains a compressible fluid with density $\rho(x,t)[\frac{kg}{m^3}]$ (in location x and time instant t), and by looking at the average velocity of the fluid over the cross section, we can find the mass balance for the volume. First, the mass flow $w[\frac{kg}{s}]$ is

$$w(x,t) = \int_A \rho v dA = \rho \bar{v} A \tag{1}$$

where $\bar{v}$ is the average velocity. Thus, for this simple one-dimensional problem, the mass balance is found to be

$$\frac{\partial \rho}{\partial t} = -\frac{1}{A}\frac{\partial w}{\partial x} \tag{2}$$

This is now in the form of a differential equation that describes the dynamics of the density in the volume. Instead, we would like to make a change of variables to pressure, and this is achieved by considering the equation, $dp = (\beta/\rho)d\rho$ where $\beta[Pa]$ is the bulk modulus. This gives

$$\frac{\partial p}{\partial t} = -\frac{\beta}{A}\frac{\partial q}{\partial x} \tag{3}$$

where q is the volumetric flow rate $[\frac{m^3}{s}]$. To find an equation for the flow rate, q, we consider the momentum balance for the same control volume, which reduces to

$$\frac{\partial w}{\partial t} = -A\frac{\partial p}{\partial x} - A\frac{\partial}{\partial x}\int_A \rho v^2 dA - F + A\rho g\cos(\alpha) \tag{4}$$

where the term α is defined as the angle between the positive flow direction and gravity $g[\frac{m}{s^2}]$. Fdx is the friction force acting on the volume. Now, assuming that the change $\frac{\partial}{\partial x}\int_A \rho v^2 dA$ is small, we neglect this term and treat the density as a constant to obtain the equation for the volumetric flow rate

$$\frac{\partial q}{\partial t} = -\frac{A}{\rho_0}\frac{\partial p}{\partial x} - \frac{F}{\rho_0} + Ag\cos(\alpha(x)). \tag{5}$$

To summarize, the continuous differential equations describing the hydraulic transmission line are given by equations (3) and (5).

2.2 Discretized Simulation Model With Variable Complexity

The transmission line model derived in the previous section is in the form of two coupled partial differential equations. For simulation, this has to be discretized in both time and space, so we choose a simple finite volumes method and apply the differential equations to the average pressures and flows of each control volume. The flows and pressures are defined on a staggered grid, with pressures defined at the center of the control volumes and flows at the boundaries, as shown in Figure 2.

Boundary Conditions

Boundary conditions for the model are the different external inputs; the mud pump flow q_p, the back pressure pump flow q_{bpp}, the influx from the surroundings q_f and the control signal u_c. The choke flow is modeled by the orifice equation, $q_c = K_c g_c(u_c)\sqrt{\frac{\Delta p}{\rho}}$, where K_c is a choke constant and $g_c(u_c)$ gives the choke opening, between 0 and 1, as a function of the control signal, u_c.

Parameterization of Physical Quantities

All physical quantities on the right hand side of (3) and (5) have to be parameterized as a function of the spatial coordinate x, so that control volume i has its own cross section A_i, density ρ_i, bulk modulus β_i, height difference Δh_i and frictional pressure loss $F_i = F(q_i, d_i, l_i, \rho_i, \mu_i)$ where $d_i[m]$ is the inner diameter of the drill string (or hydraulic diameter of annulus) in cross section i, $l_i[m]$ is the length of volume i and μ_i $[\frac{kg}{sm}]$ is the viscosity in volume i.

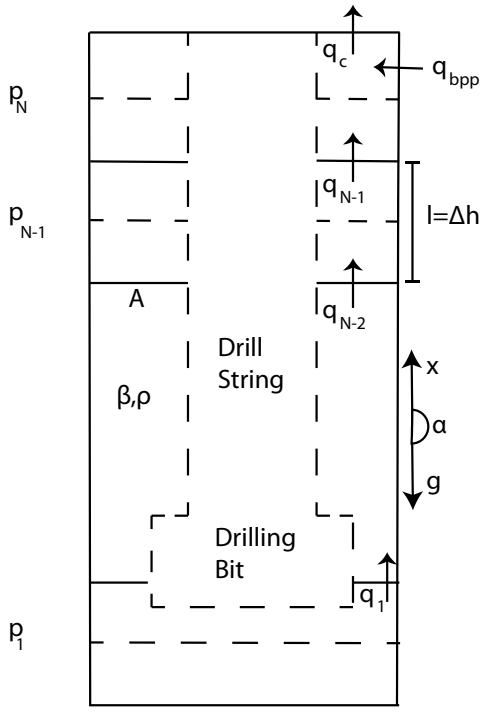

Figure 2: Control volumes and geometry for discretized system.

Complete Simulation Model

Combining all of this, we can now write down the entire simulation model for an arbitrary number of control volumes N

$$
\begin{aligned}
\dot{p}_{1d} &= \frac{\beta_{1d}}{A_{1d}l_{1d}}(q_p - q_{1d}) \\
\dot{p}_{2d} &= \frac{\beta_{2d}}{A_{2d}l_{2d}}(q_{1d} - q_{2d}) \\
&\vdots \\
\dot{p}_{Nd} &= \frac{\beta_{Nd}}{A_{Nd}l_{Nd}}(q_{(N-1)d} - q_{bit}) \\
\dot{q}_{1d} &= \frac{A_{1d}}{l_{1d}\rho_{1d}}(p_{1d} - p_{2d}) - \frac{F_{1d}A_{1d}}{\rho_{1d}l_{1d}} + Ag\frac{\Delta h_{1d}}{l_{1d}} \\
&\vdots \\
\dot{q}_{(N-1)d} &= \frac{A_{(N-1)d}}{l_{(N-1)d}\rho_{(N-1)d}}(p_{(N-1)d} - p_{Nd}) - \frac{F_{(N-1)d}A_{(N-1)d}}{\rho_{(N-1)d}l_{(N-1)d}} + Ag\frac{\Delta h_{(N-1)d}}{l_{(N-1)d}} \\
\dot{q}_{bit} &= \frac{2A_{Nd}A_{1a}}{A_{1a}\rho_{Nd}l_{Nd} + A_{Nd}\rho_{1a}l_{1a}}\Big((p_{Nd} - p_{1a}) - F_{bit} + \frac{g(\rho_{Nd}\Delta h_{Nd} - \rho_{1a}\Delta h_{1a})}{2}\Big) \\
\dot{p}_{1a} &= \frac{\beta_{1a}}{A_{1a}l_{1a}}(q_{bit} - q_{1a} + q_f) \\
&\vdots \\
\dot{p}_{Na} &= \frac{\beta_{Na}}{A_{Na}l_{Na}}(q_{(N-1)a} - q_c + q_{bpp}) \\
\dot{q}_{1a} &= \frac{A_{1a}}{l_{1a}\rho_{1a}}(p_{1a} - p_{2a}) - \frac{F_{1a}A_{1a}}{\rho_{1a}l_{1a}} - Ag\frac{\Delta h_{1a}}{l_{1a}} \\
&\vdots
\end{aligned}
\tag{6}
$$

$$\dot{q}_{(N-1)a} = \frac{A_{(N-1)a}}{l_{(N-1)a}\rho_{(N-1)a}}(p_{(N-1)a} - p_{Na}) - \frac{F_{(N-1)a}A_{(N-1)a}}{\rho_{(N-1)a}l_{(N-1)a}} - Ag\frac{\Delta h_{(N-1)a}}{l_{(N-1)a}}$$

Here, the subscripts a, d refer to annulus and drill string, respectively. We also define the influx from the surroundings to enter into volume 1 on the annulus side. This is because the rest of the annulus is usually cased in concrete so there should be no influx into the other volumes. Finally, the equation for the drill bit flow q_{bit} is described in a similar manner to what was done in [31]. Here however, we use only the lower-most volumes on each side of the bit to calculate the pressure and weight difference.

2.3 Friction Model

The drilling mud is a highly complex fluid that does not exhibit the classical Newtonian behavior. It is known to exhibit a so called yield stress, meaning that it takes a certain pressure gradient to initiate flow. We consider the implications of the non-Newtonian behavior in this paper.

Bingham Plastic Rheological Model

In this paper, the Bingham plastic model is used to describe drilling mud flow model, which incorporates a yield stress

$$\tau = \tau_0 + \mu\frac{\partial v}{\partial y} \tag{7}$$

where $\tau_0[Pa]$ is the yield stress and μ is the viscosity.

Frictional Pressure Losses in Steady, Laminar Flow

A classical friction model including a static break-away force is used to model the yield stress behavior of the system. This model takes the following form

$$F(v, F_e) = \begin{cases} F_f(v) & v \neq 0 \\ F_e & v = 0\, and\, |F_e| < F_s \\ F_s sgn(F_e) & otherwise \end{cases} \tag{8}$$

The idea is that we look at the pressure difference over a control volume, $F_e = \Delta p - \rho g \Delta h$, and see if this is larger than the yield pressure, F_s. If it is not, the friction force will exactly match the external pressure force. If it is larger however, there will be a non-zero flow, and we can calculate the pressure loss as $F_f(v)$, given by constant yield pressure plus a term proportional to flow rate for viscous friction; $F_f(v) = k_1 + k_2 v$. This model provides enough damping for low flow rates. Figure 3 shows the pressure difference from mud pump to control choke and the mud pump flow for an experiment carried out at UllRigg - a full scale experimental offshore type drilling rig located at International Research Institute of Stavanger, Norway. The mud pump and the choke are at approximately the same height, so the pressure difference between them is dominated by friction. Therefore, the graphs of Figure 3 provides us with the frictional loss as a function of flow rate. From this experiment, we can also find the pressure drops in the annulus and drill string separately by looking at the down hole measured pressure and correcting for the height difference. These pressure losses as a function of flow rate can be seen in Figure 4. Notice that the pressure drops in the drill string also include the valve at the drill bit, which typically has a high pressure drop.
Figure 4 suggests that the pressure losses are linear functions of the flow rate for a large range of flows, which fits well with the standard theory on friction factors for laminar flow. What is more important, is that we do not see a build up in pressure difference that is needed to overcome a static break-away force. Instead, one might think of this as the pump pushing the solid gel with a constant force until the gel yields and begins to flow. This is what inspired the final model of the mud as a substance that can change between different phases dependent on external influence, governed by the simple state diagram in Figure 5.

To conclude, the influence of friction can be expressed in the following way. In the zero flow state, there is no change anywhere in the system, and we are in a steady state. When flow is initiated, there is a resistance against the flow, but this is due to the solid state of the gel and does not lead to an increased pressure anywhere in the system. When the gel breaks down and starts to flow as a fluid, in the laminar flow regime there would be a friction force that is linear in the flow rate, $F_f(v) = k_1 + k_2 v$. To model this linear friction force, we add a quite small constant k_1 to increase the damping and stability of the system for low flow rates. The second part, $k_2 v$, can be modeled using standard Newtonian friction factor correlation $f = \frac{16}{Re}$ where Re is the Reynolds number of the flow. The tuning parameters will then be the physical properties of the mud, especially the viscosity, which can be obtained by substituting the Reynolds number and friction factor into the equation for the pressure loss to give the linear expression

$$\Delta p = \frac{32\mu L v}{R^2} \tag{9}$$

where R is the radius of the cylindrical pipe.

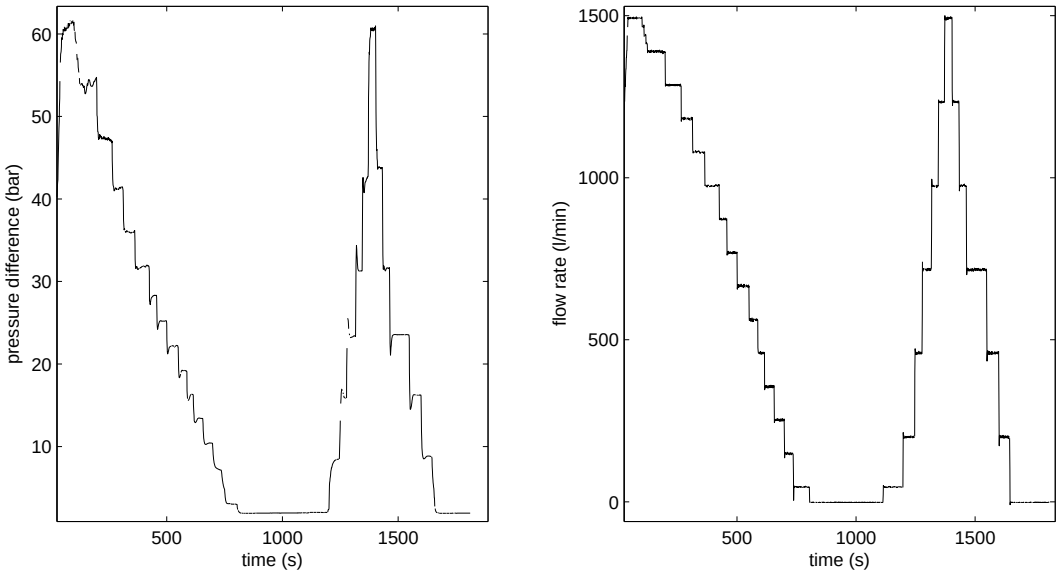

Figure 3: Pressure difference and flow rate for experimental data.

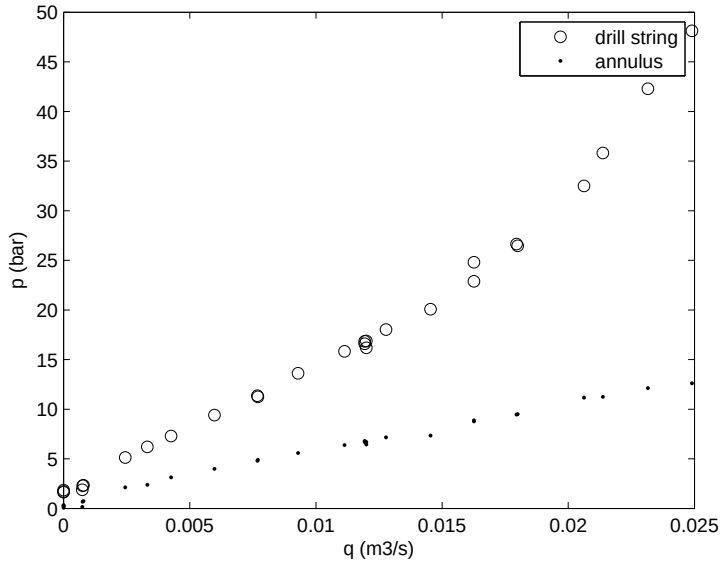

Figure 4: Pressure drops in drill string and annulus, UllRigg data.

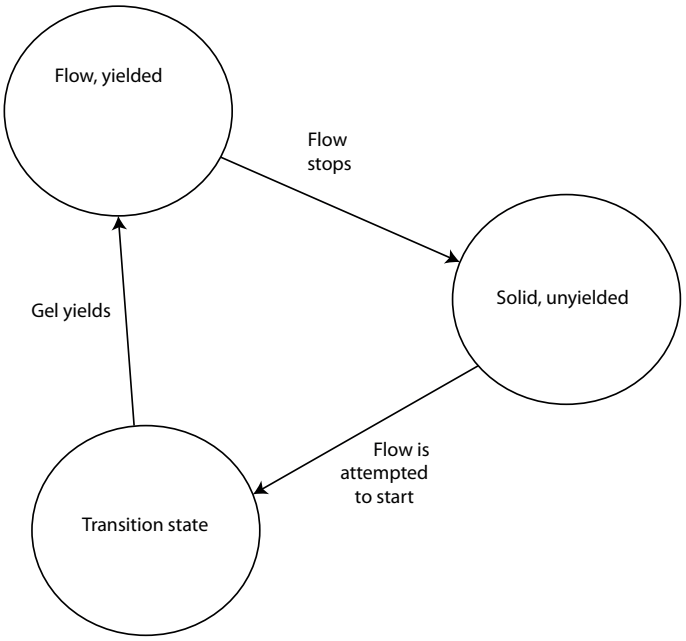

Figure 5: State diagram for gel/liquid behavior.

Effects of Different Geometries

In this paper we are interested in taking a unified approach towards different geometries in friction factor similar to what is done in [32]. The paper finds a unified solution by letting the friction factor for the laminar case be $f = \frac{16}{Re^*}$, where Re^* is a generalized Reynolds number defined by $Re^* = \frac{\rho v^{2-n^*} r_h^{n^*}}{2^{n^*-3} K^*}$. Here, r_h is the hydraulic radius and is given by

$$r_h = \begin{cases} \frac{d}{4} & cylinder \\ \frac{(d_2-d_1)}{4} & concentric\,annulus \end{cases}$$

n^* and K^* have very specific meaning, but in the simple case of the Newtonian model, it suffices to say that they reduce to $n^* = 1$ and $K^* = \mu(a+b)$ where a and b are constants defining the geometry of the cross section. For a cylinder, $a + b = 1$, Re^* reduces to the familiar Re for Newtonian flow in a circular pipe. But for the concentric annulus $a + b = \frac{(1-k)^2}{1+k^2-\frac{1-k^2}{ln1/k}}$, $k = \frac{R_1}{R_2}$, and $Re^* = \frac{4\rho v r_h}{\mu(a+b)}$.

Transition to Turbulent Flow

Following the simplification and using the model from the previous subsection, it makes sense to use the generalized Reynolds number as an indicator of laminar flow and expect laminar flow whenever $Re^* < 2300$. However, by examining Figure 4, we can see that there is a transition in the friction losses in the drill string, possibly due to a transition to turbulent flow. This seems to happen at a flow rate of around $q = 0.0175 \frac{m^3}{s}$. Using the density and estimated viscosity for the mud used in this experiment, this can be translated into a critical Reynolds number for the end of laminar flow. However, the critical Reynolds number is probably quite empiric and subject to other conditions of the flow, especially the inlet conditions. During the transition phase, the friction factor is highly uncertain, and neither equations for laminar nor turbulent flow will be accurate. One proposed approach is to use a linear function, $f = a_f Re + b_f$, to describe the friction factor in this phase, where $f(Re_{crit}) = \frac{16}{Re_{crit}}$ and $f(Re_{fully\,turbulent})$, given in the next section, are used to find the constants a_f, b_f. Still, one would have to determine the Reynolds number at which the flow is fully turbulent.

Fully Turbulent Flow

For the case of fully turbulent flow, one usually relies on empirical or semi-empirical models for calculating the friction factor. The most celebrated one is the Colebrook equation:

$$\frac{1}{\sqrt{f_D}} = -2log_{10}(\frac{\delta/d_h}{3.7} + \frac{2.51}{Re\sqrt{f_D}}) \tag{10}$$

This equation takes into account the roughness of the pipe through the constant δ. Notice that the subscript D refers to the fact that this is the Darcy friction factor, which is easily related to the Fanning friction factor by $f = 4f_D$ [33]. This is an implicit equation and can be solved by a simple iterative procedure. However, there are several explicit approximations to this equation, in particular the one due to Haaland, [34]:

$$\frac{1}{\sqrt{f_D}} = -1.8log_{10}\Big[\big(\frac{\delta/d_h}{3.7}\big)^{1.11} + \frac{6.9}{Re}\Big] \tag{11}$$

The Haaland equation is accurate enough and better suited for the implementation in a simulator program. To calculate the frictional pressure losses, the state diagram Figure 5 is first consulted. If we are in the transition state, in the simulations presented here, we just wait for the gel to yield. If, on the other hand, we are in the flowing state, the Reynolds number is first calculated to indicate the flow regime. Then, the friction factor is calculated as described in the previous subsections, and via this friction factor, we find the pressure drop.

2.4 New Mud Circulation

We approach the scenario of circulating in a new type of mud by tracking the front of the new mud as it travels through the system. This front divides a control volume into two distinct parts, which means that we do not consider mixing of the two types of mud. The following model is proposed for tracking the front within a control volume

$$\begin{aligned}
\dot{p}_{v1} &= \frac{\beta_1}{Al_1}(q_1 - q_f) + \frac{q_f\rho_1 g}{2A} - F\frac{q_f}{2lA} \\
\dot{q_f} &= \frac{2A}{l\bar{\rho}}(p_{v2} - p_{v1}) - F\frac{A}{\bar{\rho}l} + gA \\
\dot{p}_{v2} &= \frac{\beta_2}{Al_2}(q_f - q_2) + \frac{q_f\rho_2 g}{2A} - F\frac{q_f}{2lA}
\end{aligned} \tag{12}$$

Here, again, F is the pressure drop due to friction, and has also been included to reflect the fact that when the midpoint of the control volume shifts, there is also a pressure change due to a different friction drop. The multiplication by $\frac{1}{2}$ reflects the fact that for a certain expansion of the length of a control volume, the midpoint is shifted by half of this expansion. $\bar{\rho}$ is an average density defined by $\bar{\rho} = \frac{\rho_1 l_1 + \rho_2 l_2}{l}$ and q_f describes the speed of the front by $q_f = v_f A$. x_f denotes the distance the front has travelled into the control volume, and evolves according to $\dot{x_f} = q_f/A$. Thus $l_1 = x_f$ and $l_2 = l - x_f$. Notice that in this case, there is actually no flow going out of volume one and no flow going into volume two, so the terms q_f actually describe the changes in volumes one and two, $q_f = \dot{V}_1 = -\dot{V}_2$.

Care must also be taken to ensure that we calculate q_1 and q_2 correctly. The issue here is just to get the right size of the control volumes where these flows are defined, and this is solved by introducing the new lengths $\bar{l_1}, \bar{l_2}$ defined by $\bar{l_1} = \frac{l_1 + l}{2}$ and $\bar{l_2}$ in the same way.

2.5 Vertical Motion of Drill String

The scenario of moving the drill string vertically in the well is something that might arise in two different ways; heave and tripping. Tripping (in or out) is the controlled movement of the drill string in the well, which can be done for various purposes. Heave is the oscillatory motion of the drillstring along the well that occurs when drilling from a floater. During connections, when the heave compensation is deactivated, the drillstring is in slips and follows the vertical oscillatory motion of the floater due to waves (heave).

To model the vertical motion of the drill string, an additional dynamic variable, x_d is considered. This variable keeps track of the current position of the drill bit, and is governed by the dynamic equation $\dot{x_d} = v_d$ where v_d is the speed of the drill bit, taken as an exogenous signal. Using v_d and x_d, we can modify the frictional pressure losses as well as the dynamics of the pressures and flows surrounding the actual drill bit.

Changes in Drill String Dynamics

The control volumes are moving with the speed of the drill string, so the transport of any quantity over the cross sections is the same as before, as in equations (3), and (5).

Changes in Annulus Dynamics

If we consider the control volumes containing the mud in the annulus region, they will consist of the fixed walls of the well, which are not moving, as well as the moving inner cylinder. Although there is no transport of any quantity over this moving

boundary, the relative velocity between the fluid inside and the walls of the inner cylinder changes, which causes the pressure drop due to friction to change as well. To include this in the model, we look at the described friction factor in section 2.3.
In this paper, all derivations are actually done by introducing a slip velocity $v_0 = \frac{1}{h}\int_h v_w ds$, where h is the contour of the cross section and v_w is the slip velocity at the wall. Now, interpreting this in a slightly different way by assuming no slip, but letting the actual wall of the inner cylinder move with a constant speed v_d, we can find v_0 as $v_0 = \frac{R_1}{R_2}v_d$, reflecting the fact that only the inner cylinder is moving. Using this, we can now find the Reynolds number as $Re^* = \frac{4\rho(v-u_0)r_h}{\mu(a+b)}$, and calculate the pressure losses as before.

Another issue that needs to be addressed is what happens to the control volume which the bottom of the drill string is currently in. As the drill string moves up and down, the volume of this control volume will change, and the pressure directly outside of the drill bit will change, affecting the flow through the drill bit, q_{bit}. The change in the size of control volume can be modeled by keeping track of the distance moved by the drill bit and then calculating the pressure change as

$$\dot{p} = \frac{\beta}{V}(q_{in} - q_{out} - v_d A_d) \tag{13}$$

where q_{in} refers to the sum of all flows into the volume, i.e. $q_{\text{in}} = q_{bit} + q_f + q_a(i-1)$ and v_d is defined positive upwards so that $v_d A_d = \dot{V}$. The change in pressure outside of the drill bit can also be modeled by keeping track of the distance moved by the drill bit and calculating the pressure at the current bit position. This pressure will then determine the dynamics of q_{bit}.

2.6 Rotation of Drill String

For our purposes we need a model that is only concerned with the change in frictional pressure losses. Using the empirical and semi-empirical relationships, we can calculate the new pressure losses in both the drill string and the annulus given the rotational speed of the drill string.

Changes in Drill String Pressure

For laminar flow, [35] found the empirical relationship

$$f_D = 31\frac{Re_\omega^{0.16}}{Re} \tag{14}$$

where the rotational Reynolds number is defined as $Re_\omega = \frac{d\rho v_\omega}{\mu}$, in which v_ω is the azimuthal speed of the rotating pipe, $v_\omega = \omega R$, and ω is the rotational speed of the pipe. This expression for the friction factor is claimed to be valid for $500 < Re < 1500$ and $500 < Re_\omega < 5000$.

Changes in Annulus Pressure

Ahmed et al [36] used extensive data from four different wells during actual drilling operations together with dimensional analysis techniques to find the model

$$\begin{aligned}\text{PLR} &= \frac{(dP/dL)_\omega}{(dP/dL)_{\omega=0}} \\ &= 0.36\big(13.5 + \frac{\tau_0}{\rho v^2}\big)^{0.428} \times \epsilon_{av}^{0.158} \times Ta^{0.0319} \times n^{0.054} \times Re_{eff}^{0.042} \times k(\frac{1}{k} - 1)^{-0.0152}\end{aligned} \tag{15}$$

Stated in words, the ratio of the pressure loss with rotation to the pressure loss without rotation is defined as a function of several physical and geometrical properties. Here, τ_0 is the yield stress of the fluid, ϵ_{av} $[\frac{1}{m}]$ is the average eccentricity of the well, Ta is the Taylor number defined in (17), n is fluid behaviour index, Re_{eff} the effective Reynolds number and k the ratio of the diameters. These quantities are defined by

$$\epsilon_{av} = \frac{2E}{d_2 - d_1}\frac{L}{\Delta h} \tag{16}$$

where E is the eccentricity and is recommended to be 50% for a straight well, and larger for an inclined one. Δh is the change in elevation, equal to L for a straight well.

$$Ta = \frac{d_1\,(d_2 - d_1)^3}{16}\left(\frac{\rho\omega}{\mu}\right)^2 \tag{17}$$

$$Re_{eff} = \frac{8\rho v^2}{\tau_{wall}} \tag{18}$$

where τ_{wall} is the wall shear stress.

3 Simulation Results and Accuracy Analysis

In this part, simulation results are presented. For most of the simulations, specific scenarios are recreated for which experimental data from UllRigg tests is available. The data sets include measurements of choke flow, choke opening, mud pump flow, back pressure pump flow, mud pump pressure, choke pressure as well as a down-hole pressure sensor. In addition, the position of the drill string and rotation rate are measured, and used for the scenarios of heave and rotation. The mud pump flow and control choke opening are considered as external signals for the simulations, and the pressure estimates from the simulated model are compared to the measured pressures.

3.1 Friction Model

The frictional pressure losses are generally a function of the fluid velocity, so for purposes of verifying, and tuning our model, one of the experimental data sets in which the velocity varies over a large region is used. In this data set, the mud pump flow is stepped up and down between $1500\frac{l}{min}$ and $0\frac{l}{min}$ while the control choke is kept open at 100%. Using these two signals from the data set, the scenario was simulated, and the resulting pressure estimates are compared with the measured pressures in Figure 6. The applied mud pump flow rate, $q_p = \omega_p V_{lps}$, where V_{lps} is the volume it can move in each stroke, is illustrated in Figure 3. We can see that the steady state pressures match the data fairly well.

The number of control volumes is not important for capturing the steady state pressures or the restart of mud flow, but it does play a role when it comes to the speed of pressure waves traveling the system. As we can see from Figure 7, a lower order system reacts more slowly, and during the fast transients, the estimated pressure is somewhat erroneous. Moreover, it is evident that the difference between $N = 10$ and $N = 50$ is small, and even the lowest order, $N = 2$, is capable of reasonably well reproducing the dynamics, although it lags and introduces a small time delay in the estimate of the pressure.

3.2 Vertical Motion of Drill String

For these experiments, the drill string was moved periodically up and down with relatively high frequency while the mud pump flow was turned off and the choke fully opened. Measurements of the relative drill string position was used to estimate the velocity of the drill string. A plot of the measured relative position together with estimated velocity is given in Figure 8.

Simulation results compared to UllRigg data are shown in Figure 9. A note to these simulations is that the mud pump is actually turned off and the back pressure pump is turned on, thus the pressure dynamics of the drill string are really not interesting. In other words, there is no externally forced flow through the entire system, just around the choke.

As we can see, the main dynamics are captured through the described model. The phase of the pressure fluctuations is correct and the timing of the fluctuations is very good for the drill bit pressure.

Figure 10 shows how the number of control volumes affects the simulations. We can see that for $N = 10$ and $N = 50$ the differences are small; but in this case, the lowest order model is not performing well. Therefore, using a model with higher number of control volumes is recommended for pressure control design subject to the heave motion.

3.3 Rotation of Drill String

An experiment was done running the system with constant mud pump flow and fully open choke, while the drill string was rotated with different rotation rates. A measurement of this rotation rate was taken, which is used as an input signal for the simulations. Simulation results compared to UllRigg data are presented in Figure 11. We can see that the semi-empirical models give a fairly good estimate of the actual dynamics. In this simulation, the first pressure peak corresponds to a rotation rate of $100RPM$ whereas the second and third correspond to a rotation rate of $150RPM$, see Figure 12.

To see how the number of control volumes affect the results, this scenario was simulated with different order models, and the results can be seen in Figure 13. It is clear that the lowest order model has quite a large error when compared to the higher order models. We show in the next section that models of reduced complexity can be obtained by the method of frequency-weighted balanced model reduction.

4 Frequency-Weighted Balanced Model Reduction

Frequency-weighted balanced model reduction is a well-known tool that applies to linear systems. The method basically reduces complexity by removing dynamics that are insignificant to the input-output behavior of the model. We refer the reader to [37] for a basic introduction to frequency-weighted balanced model reduction.

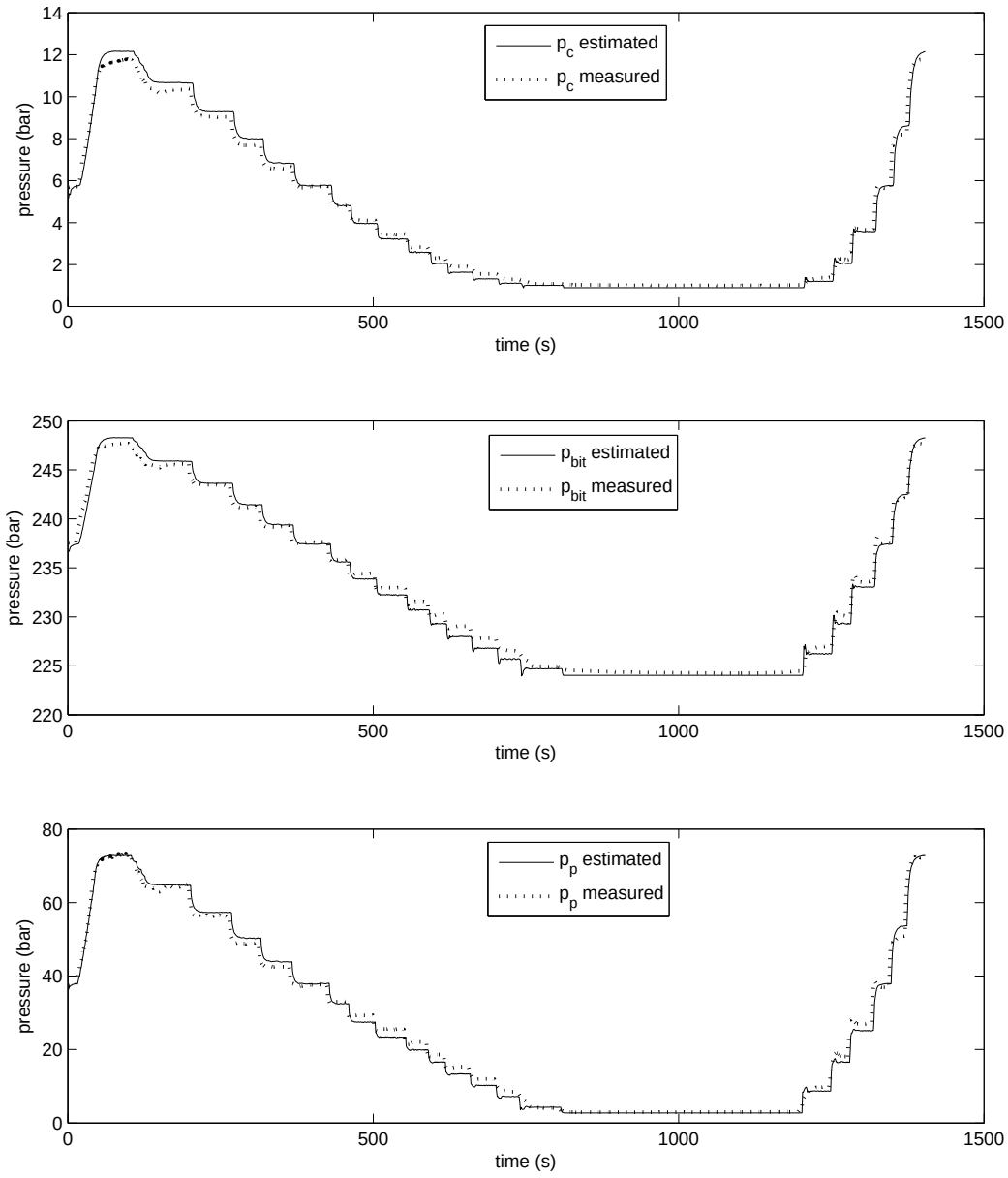

Figure 6: Measured and estimated pressure for stepping of mud pump flow.

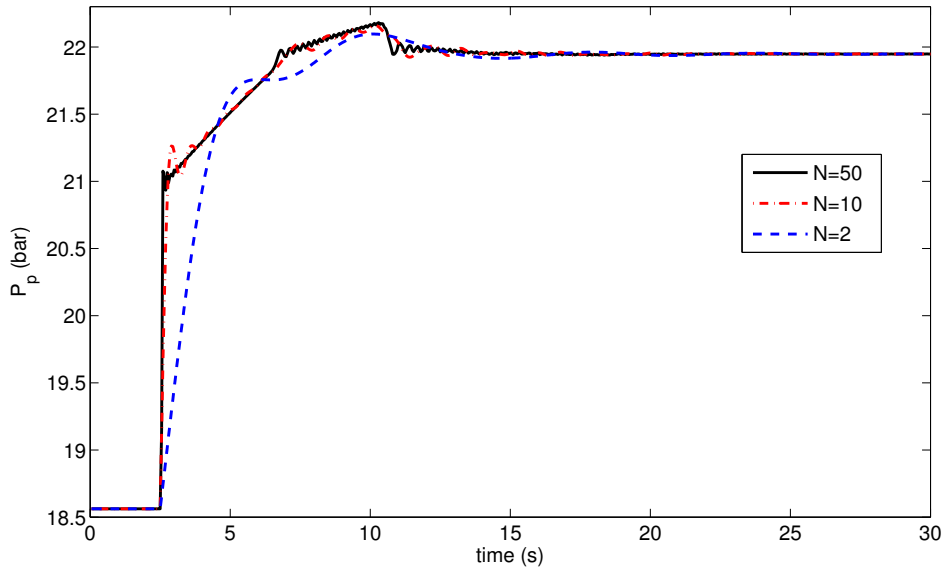

Figure 7: Step in input mud flow rate, different number of control volumes.

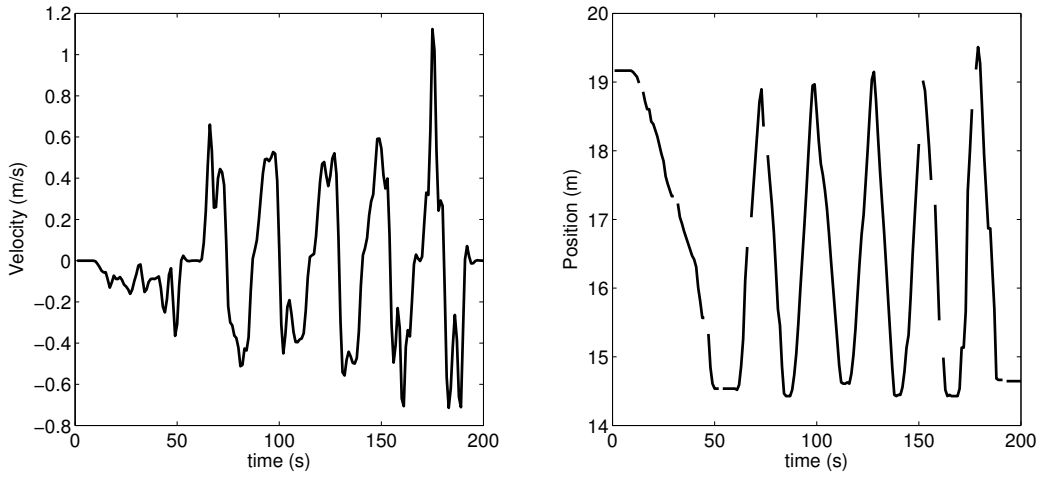

Figure 8: Position and velocity for heave emulation, UllRigg.

To apply this to the described system, it is necessary to have it in a linear form. Our friction model might cause problems for this formulation, but as we have seen at least in the laminar case, the friction loss is actually a linear function of the flow rate. Now, by defining the system input as $u = \begin{bmatrix} q_c & v_d \end{bmatrix}^T$, and disregarding the disturbance q_f, the model is in the form

$$\dot{x} = Ax + Bu \tag{19}$$

for appropriately defined state vector x and matrices A and B. Since p_{bit} is the most important variable to predict, we select C such that the measurement equation

$$y = Cx \tag{20}$$

corresponds to $y = p_{bit}$. The system consisting of (19) and (20) is now a standard linear time invariant system to which the method of frequency-weighted balanced model reduction can easily be applied.

By looking at the magnitude error of the frequency response of the reduced order models in Figure 14, we see that for the relevant frequencies (around typical heave frequencies) only a few states are necessary to achieve good performance. Using a low pass frequency weight, the frequency weighted model reduction can be made to focus on obtaining good performance at low frequencies.

In this simulation, the drill string velocity is $v_d(t) = sin(\frac{\pi}{6}t)$, in which $\frac{\pi}{6}$ is a typical frequency for the heave motion on floating rigs in North sea [9, 39]. Taking the number of dynamic states as a measure of model complexity, we compare reducing

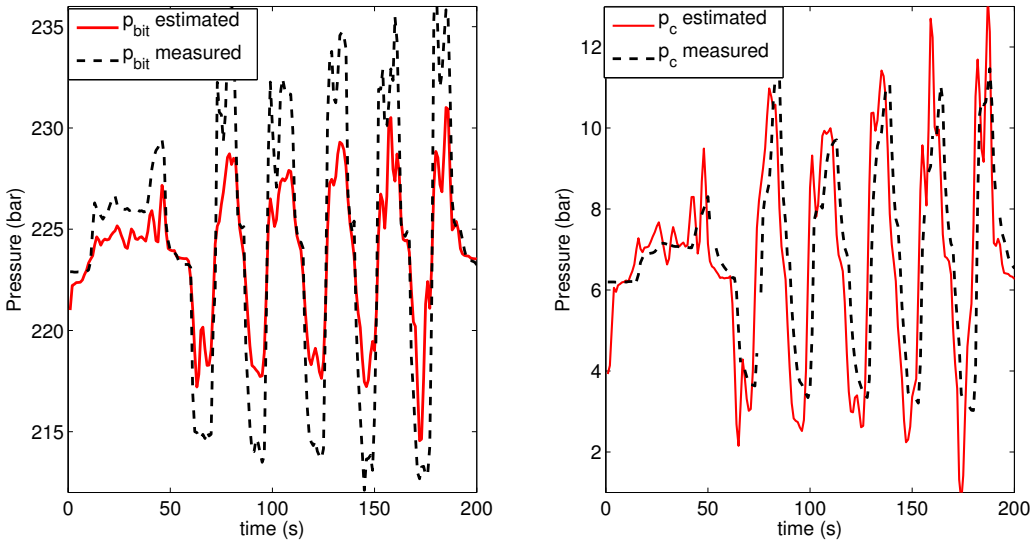

Figure 9: Pressure estimates compared to UllRigg data, heave emulation.

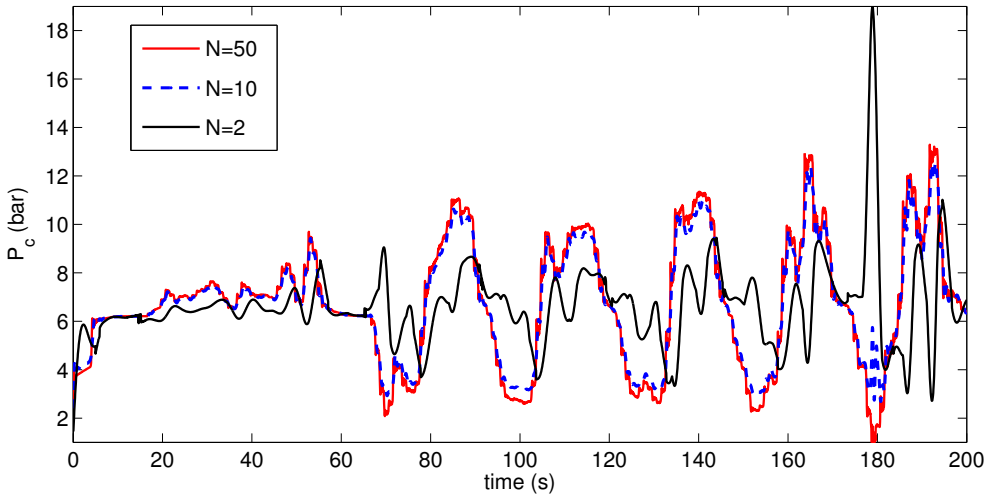

Figure 10: Heave simulation, different number of control volumes.

complexity by reducing the number of control volumes with frequency-weighted balanced model reduction. A two control volume approximation, which is a 3rd order differential equation, is compared to a 3rd order model obtained by frequency-weighted balanced model reduction applied to a 50 control volume model. The outcome is illustrated in Figure 15. Clearly the 3rd order model response matches the original system very well.

Figures 14-15 clearly show that the models obtained by frequency-weighted balanced model reduction outperform those obtained by reducing the number of control volumes.

5 Conclusions

In this paper, a dynamical model that describes the distribution of flow and pressure in a drilling fluid is derived. It has been shown that a friction model based on standard, Newtonian friction factor correlations gives a simple and accurate way of describing the pressure losses during flow, with the viscosity of the fluid as a tuning parameter. This is also suitable for a simulator program, as opposed to the non-Newtonian correlations. Still, care must be taken for zero flow, and in this case, the yield stress of the non-Newtonian drilling fluid has to be modeled. This is done by integrating the applied external forces over time until the yield boundary is achieved.

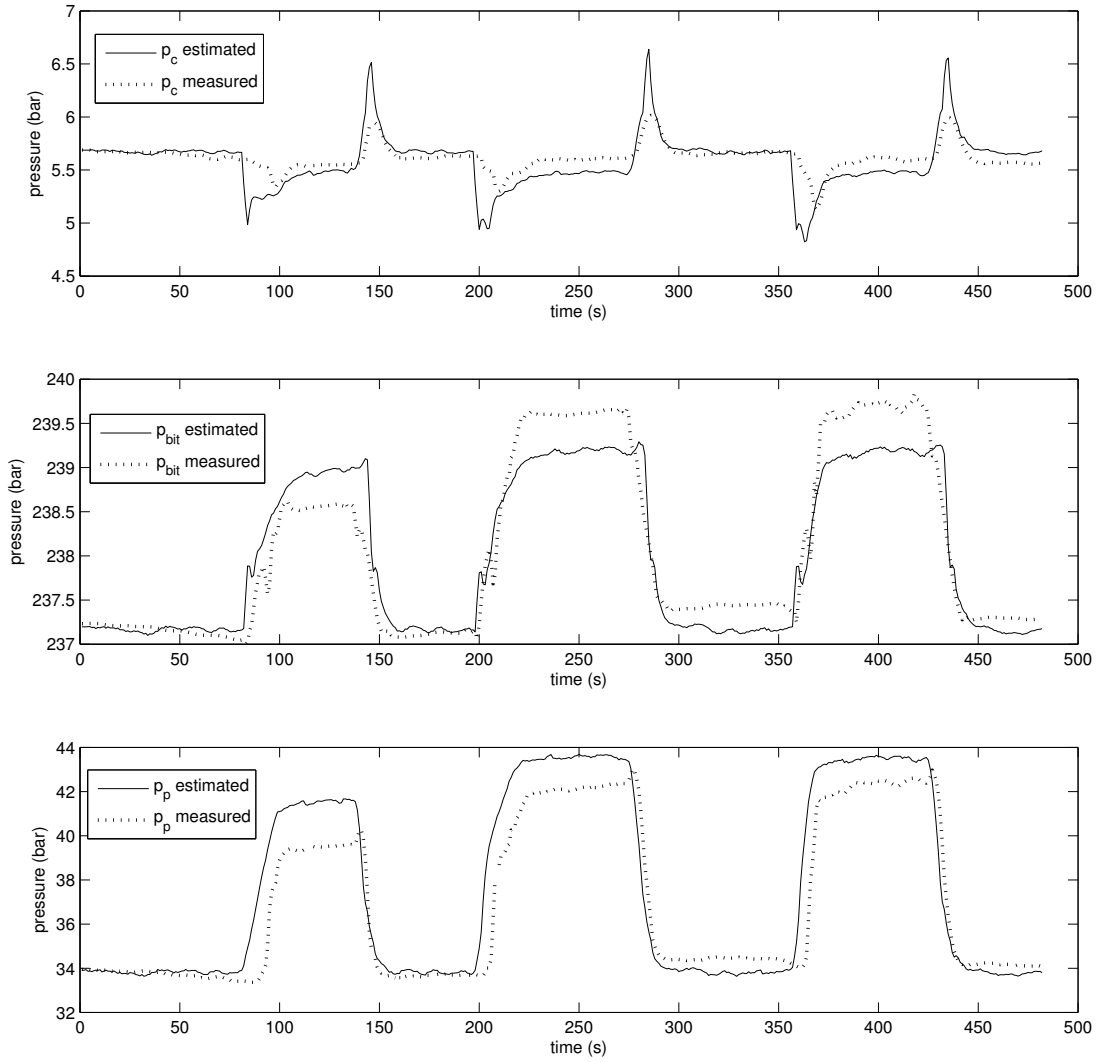

Figure 11: Estimated and measured pressure for rotating drill string.

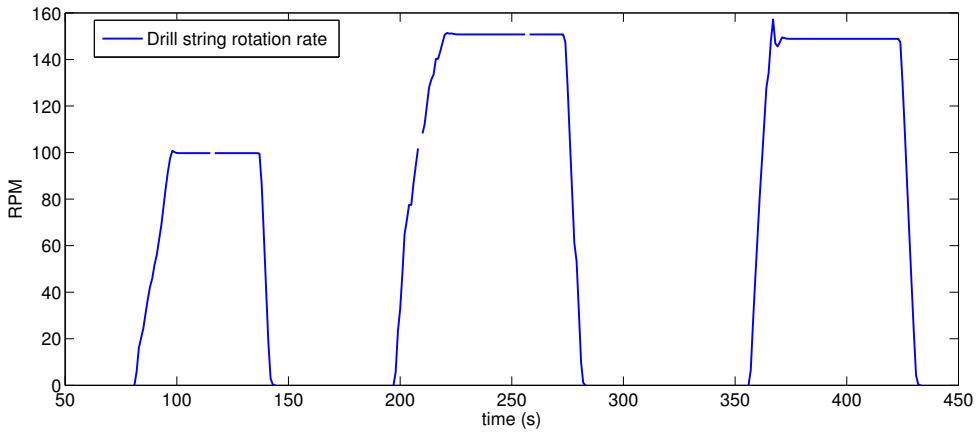

Figure 12: Drill string rotation rate.

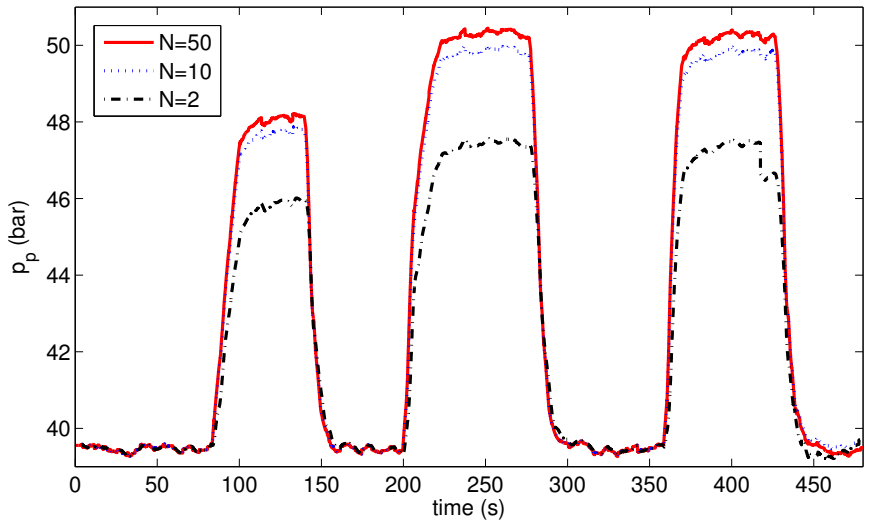

Figure 13: Rotating drill string, different number of control volumes.

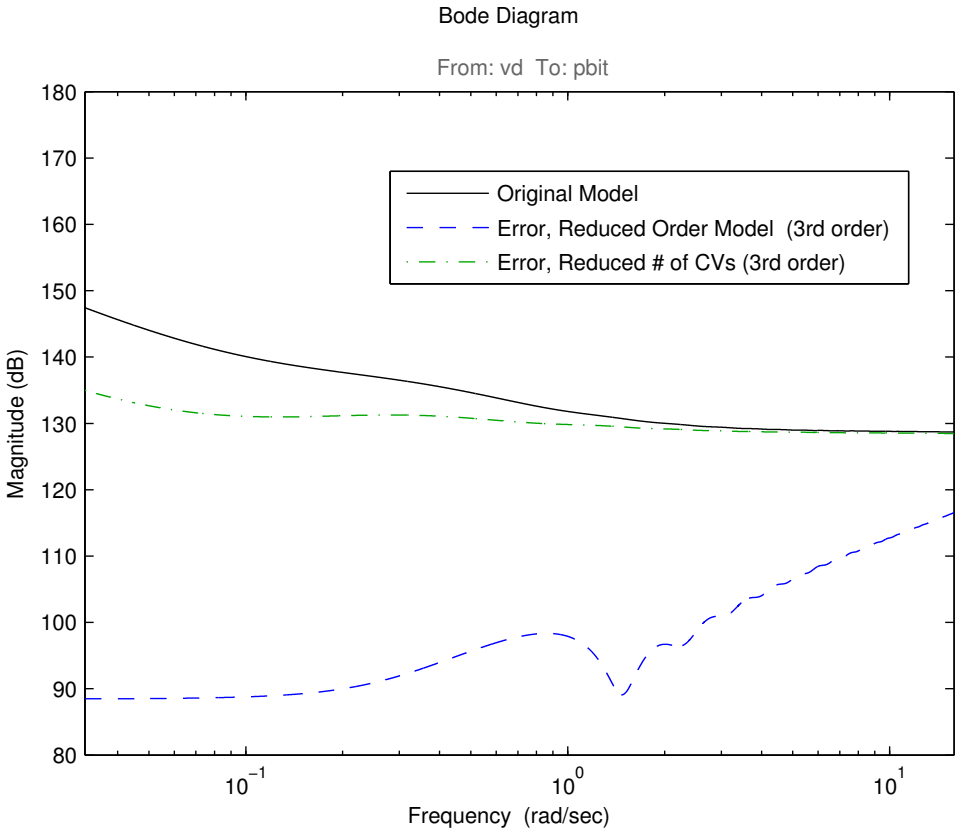

Figure 14: Magnitude of the frequency response error of the reduced order models.

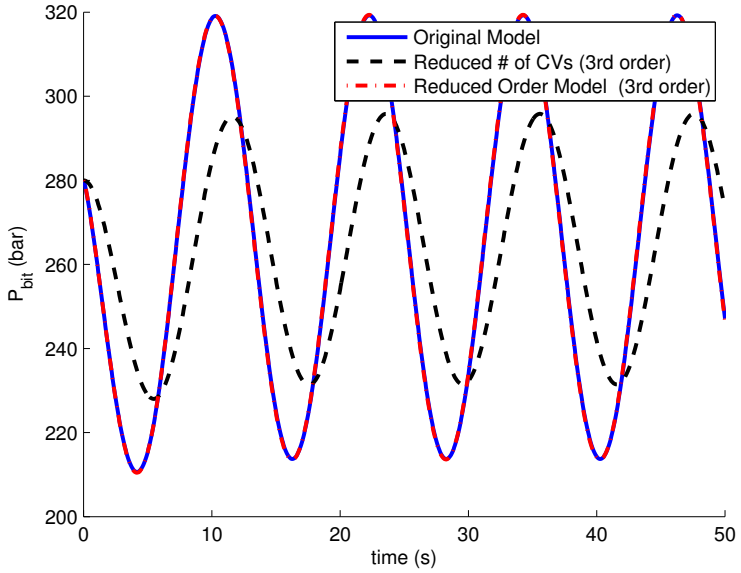

Figure 15: Comparison of control volume method and frequency-weighted balanced model reduction, 3rd order models.

The model has been validated using data from the UllRigg experimental facility for several different MPD operations. It is shown by simulation that a model of quite low order gives adequate accuracy except for the case with vertical motion of the drill string. It is shown in simulations that reduced order models based on frequency-weighted balanced model reduction outperform those obtained by simply reducing the number of control volumes.

Acknowledgments

The authors would like to thank Statoil for providing experimental data, and Dr Christian Holden of NTNU for his help in preparing the manuscript.

Bibliography

[1] B. Rehm, J. Schubert, A. Haghshenas, A. S. Paknejad, and J. Hughes, *Managed Pressure Drilling*. Gulf Publishing Company, 2008.

[2] E. van Riet, D. Reitsma, and B. Vandecraen, "Development and testing of a fully automated system to accurately control downhole pressure during drilling operations," in *SPE/IADC Middle East Drilling Technology Conference and Exhibition*, no. 85310-MS, The Society of Petroleum Engineers. Abu Dhabi, United Arab Emirates: SPE, October 2003.

[3] J. E. Gravdal, R. J. Lorentzen, K. K. Fjelde, and E. H. Vefring, "Tuning of computer model parameters in managed-pressure drilling applications using an unscented-kalman-filter technique," *SPE Journal*, vol. 15, no. 3, pp. 856–866, 2010.

[4] Ø. N. Stamnes, J. Zhou, G.-O. Kaasa, and O. M. Aamo, "Adaptive observer design for the bottomhole pressure of a managed pressure drilling system," in *IEEE Conference on Decision and Control*, 2008, pp. 2961–2966.

[5] J. Zhou, O. N. Stamnes, O. M. Aamo, and G.-O. Kaasa, "Adaptive output feedback control of a managed pressure drilling system," in *47th IEEE Conference on Decision and Control*. Piscataway, NJ, USA: IEEE, December 2008, pp. 3008–3013.

[6] J. Zhou, Ø. N. Stamnes, O. M. Aamo, and G.-O. Kaasa, "Pressure regulation with kick attenuation in a managed pressure drilling system," in *IEEE Conference on Decision and Control*, Shanghai, 2009, pp. 5586–5591.

[7] G. Nygaard, L. Imsland, and E. A. Johannessen, "Using nmpc based on a low-order model for control pressure druing oil well drilling," in *8th International Symposium on Dynamics and Control of Process Systems*, vol. 8, no. 1. IFAC, 2007.

[8] O. G. H. Nygaard, "Multivariable process control in high temperature and high pressure environment using non-intrusive multi sensor data fusion," Ph.D. dissertation, Norwegian University of Science and Technology (NTNU), 2006.

[9] B. Fossli and S. Sangesland, "Managed pressure drilling for subsea applications; well control challenges in deep waters," in *SPE/IADC Underbalanced Technology Conference and Exhibition*, no. 91633-MS. Houston, Texas: The Society of Petroleum Engineers, October 2004.

[10] J. Zhou, Ø. N. Stamnes, O. M. Aamo, and G.-O. Kaasa, "Switched control for pressure regulation and kick attenuation in a managed pressure drilling system," *IEEE Transactions on Control Systems Technology*, vol. 19, no. 2, pp. 337–350, 2011.

[11] J.-M. Godhavn, A. Pavlov, G.-O. Kaasa, and N. L. Rolland, "Drilling seeking automatic control solutions," in *Proceedings of the 18th World Congress*, vol. 18, no. 1, The International Federation of Automatic Control. Milano, Italy: IFAC, September 2011, pp. 10 842–10 850.

[12] R. Rommetveit and E. Vefring, "Comparison of results from an advanced gas kick simulator with surface and downhole data from full scale gas kick experiments in an inclined well," in *SPE Annual Technical Conference and Exhibition*, no. 22558-MS. Dallas, Texas: Society of Petroleum Engineers, October 1991.

[13] A. Ansari, N. Sylvester, C. Sarica, O. Shoham, and J. Brill, "A comprehensive mechanistic model for upward two-phase flow in wellbores," *SPE Production Facilities*, vol. 9, no. 2, pp. 143–151, May 1994.

[14] J. Petersen, R. Rommetveit, and B. A. Tarr, "Kick with lost circulation simulator, a tool for design of complex well control situations," in *SPE Asia Pacific Oil and Gas Conference and Exhibition*, no. 49956-MS. Perth, Australia: Society of Petroleum Engineers, October 1998.

[15] S. A. Hansen, R. Rommetveit, N. Sterri, B. Aas, and A. Merlo, "A new hydraulics model for slim hole drilling applications," in *SPE/IADC Middle East Drilling Technology Conference*, no. 57579-MS. Abu Dhabi, United Arab Emirates: Society of Petroleum Engineers, November 1999.

[16] A. Lage, E. Nakagawa, R. Time, E. Vefring, and R. Rommetveit, "Full-scale experimental study for improved understanding of transient phenomena in underbalanced drilling operations," in *SPE/IADC Drilling Conference*, no. 52829-MS. Amsterdam, Netherlands: Society of Petroleum Engineers, March 1999.

[17] L. E. Gomez, O. Shoham, Z. Schmidt, R. N. Chokshi, and T. Northug, "Unified mechanistic model for steady-state two-phase flow: Horizontal to vertical upward flow," *SPE Journal*, vol. 5, no. 3, pp. 339–350, September 2000.

[18] A. Lage, R. Rommetveit, and R. Time, "An experimental and theoretical study of two-phase flow in horizontal or slightly deviated fully eccentric annuli," in *IADC/SPE Asia Pacific Drilling Technology*, no. 62793-MS. Kuala Lumpur, Malaysia: Society of Petroleum Engineers, September 2000.

[19] A. C. Lage and R. W. Time, "Mechanistic model for upward two-phase flow in annuli," in *SPE Annual Technical Conference and Exhibition*, no. 63127-MS. Dallas, Texas: Society of Petroleum Engineers, October 2000.

[20] K. Bjørkevoll, B.-T. Anfinsen, A. Merlo, N.-H. Eriksen, and E. Olsen, "Analysis of extended reach drilling data using an advanced pressure and temperature model," in *IADC/SPE Asia Pacific Drilling Technology*, no. 62728-MS. Kuala Lumpur, Malaysia: Society of Petroleum Engineers, September 2000.

[21] J. Petersen, K. S. Bjørkevoll, and K. Lekvam, "Computing the danger of hydrate formation using a modified dynamic kick simulator," in *SPE/IADC Drilling Conference*, no. 67749-MS. Amsterdam, Netherlands: Society of Petroleum Engineers, February 2001.

[22] C. Perez-Tellez, J. Smith, and J. Edwards, "A new comprehensive, mechanistic model for underbalanced drilling improves wellbore pressure predictions," in *SPE International Petroleum Conference and Exhibition in Mexico*, no. 74426-MS. Villahermosa, Mexico: Society of Petroleum Engineers, February 2002.

[23] K. S. Bjørkevoll, R. Rommetveit, B. Aas, H. Gjeraldstveit, and A. Merlo, "Transient gel breaking model for critical wells applications with field data verification," in *SPE/IADC Drilling Conference*, no. 79843-MS. Amsterdam, Netherlands: Society of Petroleum Engineers, February 2003.

[24] A. C. Lage, K. K. Fjelde, and R. W. Time, "Underbalanced drilling dynamics: Two-phase flow modeling and experiments," *SPE Journal*, vol. 8, no. 1, pp. 61–70, March 2003.

[25] J. Petersen, R. Rommetveit, K. S. Bjørkevoll, and J. Frøyen, "A general dynamic model for single and multi-phase flow operations during drilling, completion, well control and intervention," in *IADC/SPE Asia Pacific Drilling Technology Conference and Exhibition*, no. 114688-MS. Jakarta, Indonesia: Society of Petroleum Engineers, August 2008.

[26] C. S. Avelar, P. R. Ribeiro, and K. Sepehrnoori, "Deepwater gas kick simulation," *Journal of Petroleum Science and Engineering*, vol. 67, no. 1-2, pp. 13–22, July 2009.

[27] K. S. Bjørkevoll, D. O. Molde, R. Rommetveit, and S. Syltøy, "Mpd operation solved drilling challenges in a severely depleted hp/ht reservoir," in *IADC/SPE Drilling Conference*, no. 112739-MS. Florida, USA: Society of Petroleum Engineers, March 2008.

[28] S. Syltøy, S. E. Eide, S. Torvund, P. C. Berg, T. Larsen, H. Fjeldberg, K. S. Bjørkevoll, J. M. O. I. Prebensen, and E. Low, "Highly advanced multitechnical mpd concept extends achievable hp/ht targets in the north sea," in *SPE/IADC Managed Pressure Drilling and Underbalanced Operations Conference and Exhibition*, no. 114484-MS. Abu Dhabi, UAE: Society of Petroleum Engineers, January 2008.

[29] K. S. Bjørkevoll, S. Hovland, I. B. Aas, and E. Vollen, "Successful use of real time dynamic flow modelling to control a very challenging managed pressure drilling operation in the north sea," in *SPE/IADC Managed Pressure Drilling and Underbalanced Operations Conference and Exhibition*, no. 130311-MS. Kuala Lumpur, Malaysia: Society of Petroleum Engineers, February 2010.

[30] O. Egeland and J. T. Gravdahl, *Modeling and Simulation for Automatic Control*. Marine Cybernetics, 2002.

[31] G. Kaasa, O. Stamnes, L. Imsland, and O. Aamo, "Intelligent estimation of downhole pressure using a simple hydraulic model," in *IADC/SPE Managed Pressure Drilling and Underbalanced Operations Conference Exhibition*, no. 143097-MS. Colorado, USA: The Society of Petroleum Engineers, April 2011.

[32] W. Kozicki, C. H. Chou, and C. Tiu, "Non-newtonian flow in ducts of arbitrary cross-sectional shape," *Chemical Engineering Science*, vol. 21, no. 8, pp. 665–679, 1966.

[33] C. F. Colebrook, "Turbulent flow in pipes, with particular reference to the transition region between the smooth and rough pipe laws," *Journal of the Institution of Civil Engineers*, vol. 11, no. 4, pp. 133–156, February 1939.

[34] S. E. Haaland, "Simple and explicit formulas for the friction factor in turbulent pipe flow," *Journal of Fluids Engineering*, vol. 105, no. 1, pp. 89–90, March 1983.

[35] S. Imao, M. Itoh, Y. Yamada, and Q. Zhang, "The characteristics of spiral waves in an axially rotating pipe," *Experiments in Fluids*, vol. 12, no. 4-5, pp. 277–285, 1992.

[36] R. Ahmed, M. Enfis, H. Miftah-El-Kheir, M. Laget, and A. Saasen, "The effect of drillstring rotation on equivalent circulation density: Modeling and analysis of field measurements," *SPE Annual Technical Conference and Exhibition*, vol. 135587-MS, 2010.

[37] K. Zhou, J. C. Doyle, and K. Glover, *Robust and optimal control*. Prentice Hall, 1996.

[38] S. Skogestad and I. Postlethwaite, *Multivariable Feedback Control: Analysis and Design*. Wiley-Interscience, 2005, vol. 2nd edition.

[39] J.-M. Godhavn, "Control requirements for automatic managed pressure drilling system," *SPE Drilling Completion*, vol. 25, no. 3, pp. 336–345, September 2010.